HHS Public Access

Author manuscript

Electrophoresis. Author manuscript; available in PMC 2019 March 01.

Published in final edited form as:

Electrophoresis. 2018 March ; 39(5-6): 844–852. doi:10.1002/elps.201700308.

Determination of lipid bilayer affinities and solvation characteristics by electrokinetic chromatography using polymer-bound lipid bilayer nanodiscs

William M. Penny and **Christopher P. Palmer**

Department of Chemistry and Biochemistry, University of Montana, Missoula, MT 59803 USA

Abstract

Styrene-maleic acid polymer-bound lipid bilayer nanodiscs have been investigated and characterized by electrokinetic chromatography. Linear solvation energy relationship analysis was employed to characterize the changes in solvation environment of nanodiscs of varied belt to lipid ratio, belt polymer chemistry and molecular weight, and lipid composition. Increases in the lipid to belt polymer ratio resulted in smaller, more cohesive nanodiscs with greater electrophoretic mobility. Nanodisc structures with belt polymers of different chemistry and molecular weight were compared and showed only minor changes in solvent characteristics and selectivity consistent with changes in structure of the lipid bilayer. Seven phospholipid and sphingomyelin nanodiscs of different lipid composition were characterized. Changes in lipid head group structure had a significant effect on bilayer-solute interactions. In most cases, changes in alkyl tail structure had no discernible effect on solvation environment aside from those explained by changes in the gel-liquid transition temperature. Comparison to vesicles of similar lipid composition show only minor differences in solvation environment, likely due to differences in lipid composition and bilayer curvature. Together these results provide evidence that the dominant solute-nanodisc interactions are with the lipid bilayer and that head group chemistry has a greater impact on bilayer-solute interactions than alkyl tail or belt polymer structure. Nanodisc electrokinetic chromatography is demonstrated to allow characterization of solute interactions with lipid bilayers of varied composition.

Keywords

electrokinetic chromatography; phospholipid bilayer; nanodisc; linear solvation energy relationships; sphingomyelin

1 Introduction

In 1984, Terabe *et al.* introduced a variation of capillary electrophoresis (CE) known as electrokinetic chromatography (EKC)[1] that allowed for the separation of nonionic analytes by selective interaction with an ionic pseudostationary phase (PSP) dissolved in the background electrolyte (BGE). EKC allows for fast and efficient separations of analytes in a condensed liquid phase.

In that original report, Terabe *et al.*[1] also suggested that EKC could be used to characterize PSPs. Numerous materials have been developed as PSPs, and the solvent characteristics of a

variety of PSP materials, including micelles[2,3], polymers[4,5], vesicles[6,7], microemulsions[8,9], liposomes[10–12], bicelles[13,14] and nanoparticles[15–17] have been studied by EKC. The solvent characteristics of liposome PSPs composed of zwitterionic and anionic lipids have frequently been studied as models of lipid bilayer membranes and as a means to determine octanol water partition coefficients ($P_{o/w}$)[18–21]. In a recent publication[22], we introduced lipid bilayer nanodiscs with sytrene-maleic acid (SMA) copolymer belts as a PSP, showing that interactions between neutral analytes and bilayers composed of zwitterionic lipids could be measured and studied. Lipid nanodiscs with SMA belts were originally developed for spectroscopic analysis of membrane bound proteins[23–27].

Traditionally, bilayer-solute interactions are measured indirectly using octanol-water partition coefficients. Our previous analysis showed that retention factors with nanodiscs measured by EKC generally correlated well with $P_{o/w}$, although hydrogen bond donating solutes showed stronger interactions with the nanodiscs than expected from the general correlation. This discrepancy could be the result of structural differences between octanol and 1,2-dimyristoyl-*sn*-glycero-3-phosphocholine (14:0 PC) lipid bilayers, or could be an artifact of the use of SMA copolymer to stabilize the lipid bilayer.

In this current study, we investigate more comprehensively the effects of nanodisc chemistry and composition on solvent characteristics in order to determine if these nanodiscs can be used in future work to study small molecule, peptide and protein interactions with lipid bilayers. The first paper on nanodisc electrokinetic chromatography[22] introduced the technique, but was not able to definitely determine if the solute interaction with the nanodisc was solely or predominantly a solute-bilayer interaction. To determine the extent to which the SMA copolymer interacts with the solute probes nanodiscs are generated using systematically varied copolymer to lipid ratios, copolymer belts of different molecular weight and chemical composition, and seven different lipid compositions drawn from the lipids represented in Figure 1. The performance, selectivity and solvation characteristics of these nanodiscs are studied and compared to each other and to prior results with lipid vesicles. Some significant differences are observed as a result of changes in copolymer to lipid ratio and copolymer chemistry that may be the result of changes in the nanodisc structure or to direct interactions with the copolymer. Significant differences observed in the solvent characteristics with changes in lipid composition, as well as comparison of nanodisc solvent character with that of liposomes of similar lipid composition[28], strongly suggest that solute interactions with the lipid bilayer are dominant. The nanodisc EKC approach is demonstrated to allow the determination of subtle differences in solvent characteristics between lipid bilayer membranes of different composition.

2 Methods and Materials

2.1 Chemicals

Sodium phosphate monobasic monohydrate, sodium phosphate dibasic heptahydrate, potassium hydroxide, and hydrochloric acid were purchased from Sigma–Aldrich (Saint Louis, MO, USA). 1,2-dimyristoyl-*sn*-glycero-3-phosphocholine (14:0 PC), 1,2-dipalmitoyl-*sn*-glycero-3-phosphocholine (16:0 PC), 1-palmitoyl-2-oleoyl-*sn*-glycero-3-phosphocholine (16:0–18:1 PC), 1,2-dimyristoleoyl-*sn*-glycero-3-phosphocholine(14:1 PC), 1,2-dimyristoyl-

sn-glycero-3-phosphoethanolamine (14:0 PE), 1,2-dimyristoyl-*sn*-glycero-3-phospho-L-serine (14:0 PS), and Sphingomyelin (16:0 SM) lipids were purchased from Avanti Polar Lipids (Alabaster, AL, USA). Copolymers Xiran 30010 and Xiran 25010 (Polyscope Polymers, Geleen, Netherlands), were a gift from Stefan Scheidelaar of Utrecht University. All analytes used for analysis were obtained from either Sigma–Aldrich or ACROS Organics (Geel, Belgium).

2.2 Preparation of Xiran 30010 and Xiran 25010 copolymers

The Xiran 30010 and Xiran 25010 copolymers use the same preparation that has been described in the literature[26,29]. A 5% (w/v) solution of Xiran 30010 or Xiran 25010 is suspended in a 1 M KOH solution and refluxed for 6 h. To confirm the reaction completion FTIR analysis is employed, monitoring the shift in the carbonyl signal from 1780 to 1560 cm^{-1}. The copolymer was precipitated using 6 M HCl to create a 1.1 M HCl solution. The precipitate was washed five times with 0.1 M HCl. The copolymer was freeze-dried and stored at −20°C.

2.3 Preparation of Nanodiscs

All nanodiscs analyzed in the following experiments used the same preparative steps. Lipids dissolved in chloroform were dried using a rotary evaporator and rehydrated to 5 mM lipid concentration using a 25 mM phosphate pH 7.0 buffer. Ten freeze–thaw cycles were performed on the lipid solution using a dry ice-ethanol bath and a sonicator with a water temperature set 10°C above lipid gel-to-liquid crystalline phase transition temperature (T_m) to form multilamellar vesicles. A solution of Xiran 30010 or Xiran 25010 copolymer in 25 mM phosphate buffer is heated to 45°C to help solubilize the copolymer and then the solution is adjusted to pH 7.0. The copolymer was added to the solution, so the multilamellar solution contained the desired (w:w) copolymer to lipid ratio. The solution was then lightly vortexed for 5 min before being placed in a heated bath for 30 minutes to complete nanodisc formation. The heated bath decreased the amount of time needed for complete liposome to nanodisc conversion. Once the conversion is complete, the nanodiscs are placed in the refrigerator for storage.

2.4 Nanodisc characterization

The size and polydispersity of the nanodiscs were obtained by dynamic light scattering at 5 mM phospholipid concentration in 25 mM phosphate buffer pH 7.0 with a Malvern Zetasizer Nano ZS. All Zetasizer samples were first filtered through a 0.45 μm pore sized filters to remove any potential artifacts that would skew the results. Each synthesis was measured in three separate trials that consisted of 13–15 measurements per trial.

2.5 EKC characterization

Phosphate buffers were prepared using sodium phosphate monobasic and sodium phosphate dibasic to create 25 mM concentrations in 18 MΩ nanopure water from an EMD Millipore system (Bedford, MA, USA). A 5 mM phospholipid concentration of nanodiscs in BGE was used for all separations. Stock solutions (25 mM) of each analyte were prepared in acetone. Analytical samples were prepared from stock solutions by dilution to 250 μM in BGE so that

the injected samples contained only 1% acetone. EKC experiments were performed on an Agilent 3D CE instrument with on-column DAD controlled by Agilent Chemstation software using 50 μm id fused-silica capillaries with either 50 μm path length cells or 150 μm extended path length cells (Agilent Technologies, Santa Clara, CA, USA).

Capillaries with total length of 48.5 cm and effective length of 40 cm were flushed at the beginning of every day and every 5 runs with 1.0 M NaOH. Between injections, the capillary was flushed with acetone, nanopure water, and buffered nanodisc solution. Analytes were injected individually by 35 mBar of pressure for 5 s and detected at 225, 245, and 254 nm. All analyses were run at 15 kV applied voltage and between 18–30°C using 5 mM phospholipid concentration of nanodiscs in BGE.

The migration time and the effective electrophoretic mobility of the nanodiscs in the BGE were estimated by using the method of Bushey and Jorgenson[30] using the negative water peak as the EOF marker and the migration times of six alkyl–phenyl ketone homologs: acetophenone, propiophenone, butyrophenone, valerophenone, hexanophenone, and heptanophenone. The Excel application Solver was used to determine the nanodisc migration time that gave the maximum r^2 for the plot of log retention factor versus homolog carbon number.

The retention factors for all analytes were calculated using the following equation:

$$k=\frac{\mu_{eo}-\mu_{sol}}{\mu_{sol}-(\mu_{eo}+\mu_{PSP})}$$

Where μ_{eo} is the electroosmotic flow during the analyte run determined by the migration time of the water peak and μ_{sol} is the total (observed) electrophoretic mobility of the solute including the μ_{eo}. The μ_{PSP} is the electrophoretic mobility of the nanodiscs determined separately. The methylene selectivity was determined from the antilogarithm of the slope of the log k values versus the number of carbons in the alkyl chain of the homologous series of phenones[31]. Theoretical plate counts were calculated assuming Gaussian peaks and using the baseline peak widths as an estimate of four standard deviations. Results for different nanodiscs were compared using the appropriate Student t-test after first testing whether there was a significant difference in the variance using an F-test. LSER characterization was performed using the 32 LSER probe solutes found in supplemental Table 2, which is similar to the list used in a recent study of a latex nanoparticle PSP[32]. All solute probes were analyzed in triplicate for each LSER analysis. After measurement of *k*-values, Excel was used for multivariate linear regression to determine LSER coefficients. Each set of LSER coefficients were a result of 96 data points and the error bars in figures containing LSER data are the standard error from the multivariate linear regression. Results were considered significantly different if the standard error ranges did not overlap.

3 Results and Discussion

3.1 Nanodisc characterization

Over the course of this study, systematic changes were made to the structure and composition of the nanodiscs in order to understand how different factors affect PSP performance and selectivity. Listed in Table 1 and in Supplemental Table 1 are the nanodiscs organized by SMA copolymer belt type, SMA belt to lipid ratio and lipid composition. This allowed for a systematic comparison of nanodiscs size, electrophoretic mobility, methylene selectivity, and theoretical plate count. All measurements had 3–7 replicates.

3.1.1 SMA belt to lipid ratio—In previous work[22], nanodiscs composed of 14:0 PC were synthesized with a low SMA belt (Xiran 30010) to lipid ratio, 0.85:1.00, for the purpose of decreasing background absorbance. This yielded nanodiscs on average that were 18 to 20 nm in diameter. Here, we describe results for 14:0 PC nanodiscs synthesized using Xiran 30010 ratios of 1.00:1.00, 1.43:1.00 and 2.00:1.00. As the ratio of copolymer belt increased from 0.85 to 1.43:1.00, the diameter of the nanodiscs decreased from 20 nm to 10 nm, where it stabilized as the ratio was further increased to 2.00:1.00 (see Supplemental Table 1). Previous experiments in the literature show that 14:0 PC nanodisc will not shrink below approximately 10nm even in an excess of SMA copolymer[27]. The smaller size of the nanodiscs with higher belt to lipid ratio suggests either that there are fewer lipids per nanodisc, that the higher belt content compresses the lipid bilayer structure, or some combination of effects. Lipid bilayers are known to be fairly compressible[33]. As would be expected, the electrophoretic mobility increased as the anionic belt ratio increased and the size decreased. The nanodiscs with 1.43:1.00 and 2.00:1.00 ratio showing statistically indistinguishable values of electrophoretic mobility. Methylene selectivity is a measure of hydrophobic selectivity, meaning it is a measure of how sensitive a PSP is to slight changes in a solute's hydrophobicity[4]. As the SMA ratio increased the methylene selectivity decreased from 2.59±0.12 to 2.33±0.01. All nanodiscs using the Xiran 30010 copolymer provided efficiency of 253,000–298,000 theoretical plates with no statistically significant differences observed.

3.1.2 SMA belt structure—Nanodiscs composed of 14:0 PC lipids were synthesized with two different copolymer chemistries using 2.00:1.00 copolymer to lipid ratio and a 5 mM lipid concentration. Copolymer Xiran 30010 is 6.0 kD and contains a 2:1 styrene to maleic acid anhydride ratio, while Xiran 25010 is a larger copolymer of 10.0 kD that contains a 3:1 styrene to maleic acid anhydride ratio. These nanodiscs, with the same ratio of copolymer to lipid but different copolymer chemistry, have approximately the same diameter (Supplemental Table 1).

The results in Table 1 show no statistically significant difference in the electrophoretic mobilities with the two belt chemistries, while a statistically significant difference is observed in the methylene selectivity ($p=0.002$). The larger copolymer creates a slightly more hydrophobic environment. The efficiency was also significantly different ($p=0.001$), with the Xiran 30010 generating significantly higher plate counts.

3.1.3 Lipid composition—Seven different nanodiscs of varied lipid composition were generated from the seven lipids shown in Figure 1. Five contained uniform bilayers, and two contained mixed lipid bilayers. In order to form stable nanodiscs at all lipid compositions, a ratio of 2.50:1.00 Xiran 25010 belt to lipid ratio was required. The lipid concentration for all the nanodiscs was 5mM. This led to a range of nanodisc diameters from 8–13nm (Supplemental Table 1). Nanodiscs composed of lipids containing double bonds were larger because unsaturated lipids are not able to pack as efficiently as those with fully saturated alkyl tails. As presented in Table 1, there was a large range in electrophoretic mobilities from $-3.89\pm0.07\text{x}10^{-4}$ cm^2 $V^{-1}s^{-1}$ for 16:0 PC to $-4.12\pm0.03\text{x}10^{-4}$ cm^2 $V^{-1}s^{-1}$ for 14:0 PC. With the exception of 16:0 PC nanodiscs, it does appear that on average larger nanodiscs have lower electrophoretic mobility and a smaller migration range than smaller nanodiscs, as might be expected. Nanodiscs that contained unsaturated alkyl tails had higher methylene selectivity than nanodiscs that had saturated alkyl tails. Changes to the head group chemistry in the 0.75:0.25 16:0 PC to 14:0 PE nanodisc lead to higher methyl selectivity than would be expected for lipids with saturated alkyl tails.

3.2 LSER analysis

In order to understand what chemical interactions determine nanodisc selectivity LSER analysis was employed. LSER analysis can be represented by the following equation:

$$SP=c+eE+sS+aA+bB+vV$$

where *SP* is any property to which the free energy of the solute partitioning can be related. In the case of EKC, it is the logarithm of the solute retention factor, log *k*. The letters *V*, *E*, *S*, *A*, and *B*, are related to individual solute parameters which were cited from the literature[32] and listed in Supplemental Table 2. These specific parameters are representative of a molecule's molar volume (V), excessive molar refraction (E), dipolarity/polarizability (S), hydrogen bond acidity (A), and hydrogen bond basicity (B)[34]. The constant *c* accounts for the phase ratio and other interactions that cannot be explained by the previously mentioned solute descriptors. By using experimentally derived log *k* values and known solute descriptors the solvation characteristics of the PSP can be broken down into five different categorical interactions defined by the *v*,*e*, *s*, *a*, and *b* terms. The lower case letters represent the nanodisc solvatation characteristics derived from the nanodisc interactions with solute probes that have defined partitioning parameters.

The *v* term is used to account for cavity formation energy. A large positive *v* term indicates that the PSP is not as cohesive as the BGE and therefore less energy is required to break the interactions between the molecules of the PSP than to break the interactions between the molecules of the BGE to form a solvation pocket. The *a* term reflects a PSP's ability to accept a hydrogen bond from a solute probe relative to the BGE. Similarly the *b* term reflects the ability to donate a hydrogen bond to a solute probe relative to the BGE. It is characteristic of almost all PSPs in EKC to have a large negative *b* term because water is a superior hydrogen bond donor. The *s* term is a measure of a solute's ability to interact with the PSP or BGE through either permanent dipoles or induction effects[34]. Finally, the *e* term represents the PSP or BGE ability to interact with π or nonbonding electrons[15]; therefore a

positive term would represent having a stronger interaction with a solute's nonbonding or π electrons.

3.2.1 SMA belt to lipid ratios—LSER analysis was conducted for three nanodiscs with ratios of Xiran 30010 copolymer to 14:0 PC lipid of 1.00:1.00, 1.43:1.00, and 2.00:1.00. These LSER results were also compared to LSER results of previously published nanodisc LSER data[22] with a 0.85:1.00 SMA:lipid ratio and can be seen in Figure 2. As the ratio of Xiran 30010 copolymer to lipid was increased and the nanodisc diameter decreased, the *v* term also decreased. The nanodiscs with a larger diameter and lower belt to lipid ratio would be less densely packed than nanodiscs of a smaller diameter and higher belt to lipid ratio. Formation of a solvation pocket is more energetically favorable in the less densely packed lipid bilayer. The *a* term also decreases with increases in belt to lipid ratio, which seems counterintuitive because increasing the copolymer to lipid ratio increases the number of maleic acid carbonyls capable of accepting hydrogen bonds. However, by increasing the amount of belt used in the synthesis it appears that the lipids are packed more densely and this increase in lipid packing density may sterically inhibit hydrogen bonding between the solutes and either the lipid head groups or the water molecules surrounding the lipid head groups. Lopez *et al.*[35] suggested that solvent accessibility was an important factor in hydrogen bonding and further analysis by Tejwani *et al.*[36] determined that hydrogen bonding with water molecules is the predominate mode of hydrogen bonding in the head group region. Increasing the packing density would reduce the amount or accessibility of water molecules in the head group region thereby reducing the *a* term. It is also possible that a less densely packed bilayer would allow greater access for hydrogen bond donating solutes to interact with the carbonyl groups of the ester near the hydrophilic/hydrophobic interface. This is the region where a bulk of the hydrophilic/hydrophobic partitioning occurs[36]. The *b* term also becomes less negative as the Xiran 30010 belt to 14:0 PC ratio increases; this could be a result of the PSP becoming a less effective hydrogen bond acceptor and therefore a more efficient hydrogen bond donor. The *s* and *e* parameters did not change within standard error meaning that the SMA:lipid ratio and packing density of the lipid bilayer does not affect interactions with nonbonding, π-electrons, or polar solutes.

3.2.3 Copolymer belt composition—In order to further understand the role that the copolymer belt plays in solute-PSP interactions, LSER analyses were run on two nanodiscs with Xiran 30010 and Xiran 25010 SMA copolymer belts. The nanodiscs were generated using 5mM lipid concentrations and a belt to lipid ratio of 2.00:1.00. Comparison of the LSER results in Supplemental Figure 1 shows a statistically significant difference between the *s* and the *a* terms. The Xiran 30010 belt led to nanodiscs that had more favorable interactions with polar solutes, in addition to stronger interactions with molecules capable of donating hydrogen bonds. This change in the interactions could be a result of the chemistry of the belt or the different belts could cause structural changes to the lipid bilayer that encourage hydrogen bonding between solutes and the lipid head groups. Selectivity changes between nanodiscs with different belts can be seen in Supplemental Figure 2, where the hydrogen bond donor molecules are more retained by nanodiscs synthesized using the Xiran 30010 belt.

3.2.4 Comparisons to liposomes—To further probe whether the predominant interactions with nanodiscs are with the lipid bilayer rather than the belt polymer, LSER results were compared to liposome LSER analysis reported by Pascoe *et al.*[28] The nanodiscs used for comparison were synthesized using a 2.50:1.00 Xiran 25010 copolymer belt to 16:0–18:1 PC ratio, while the liposomes were composed of a 0.80:0.20 molar ratio of 16:0–18:1 PC to 16:0–18:1 PS. The nanodisc electrophoretic mobility was $-4.01\pm0.02\text{x}10^{-4}$ cm^2 $V^{-1}s^{-1}$ and provided a larger migration range than liposome that had an electrophoretic mobility of $-3.87\text{x}10^{-4}$ cm^2 $V^{-1}s^{-1}$. The nanodiscs' peak efficiency was also superior; Pascoe *et al.* reported that the average theoretical plates per meter (N/m) for propiophenone was 75,100[28] while the average N/m for propiophenone on the nanondiscs was 712,000. LSER results were the same within standard error for 4 of the 5 system descriptors as seen in Supplemental Figure 3. The difference in the *b* term is small but statistically significant, with the liposome value more negative than the nanodisc value. This could be a result of differences in bilayer-water interface. The nanodisc is a planar bilayer, while the liposome is a spherical bilayer. Analysis of the thermodynamics of peptide partitioning by Kim *et al.* determined that the curvature of the membrane surface may play a significant role in peptide partitioning[37], and this could apply to other solute partitioning as well. Overall, these results demonstrate that the nanodisc bilayer solvation environment is very similar to that of liposomes, suggesting that copolymer belt-solute interaction plays a minimal, if any, role in the overall nanodisc-solute interaction.

3.2.5 Lipid composition—LSER analyses were run on seven different nanodiscs with varied lipid composition to determine how structural changes in lipid head and tail chemistry affect solute-lipid bilayer interactions. Figure 3, which displays the LSER parameters for the 7 different nanodiscs, shows that the head group chemistry is much more influential in affecting bilayer-solute interactions. There were no statistically significant differences between the *v* term for the 7 nanodiscs analyzed even though there were lipids with varying alkyl tail length and degrees of unsaturation. Other studies have shown that water molecules usually only penetrate as far as the carbonyl atoms of the ester groups near the head group of the lipid[38,39], which limits the number of solute probes that interact in the hydrophobic region of the nanodisc. There are also no significant differences between the *e* terms of any of the nanodiscs, indicating that changes to the lipid structure do not affect its ability to interact with nonbonding or π electrons.

There were several significant differences between the *s* term for the nanodiscs with different lipid compositions. The *s* term for 16:0 SM was significantly more negative than the *s* terms for 14:0 PC and 16:0 PC. Since the alkyl tails for 14:0 PC, 16:0 PC, and 16:0 SM are similar lengths and saturated the difference in the *s*term must be the result of the changes to the head group chemistry. It should be mentioned that 16:0 SM was extracted from an egg and is actually 86% 16:0 SM, 6% 18:0 SM and 8% other alkyl chain variation. Unlike phospholipids, which have a glycerol backbone, sphingomyelin contains a sphingosine backbone and as a result it contains two polar groups: one hydroxyl and one amide[40], at the hydrophobic/hydrophilic interface. Both are capable of hydrogen bonding. According to simulations, 57% of sphingomyelin molecules intramolecularly hydrogen bond creating essentially a six-membered ring[40]. A side effect of this intramolecular hydrogen bond is that

it reduces the water hydration in the head group region of the lipid. Sphingomyelin nanodiscs are less capable of interacting with polar solutes because the polar region is less hydrated[40], corresponding to a more negative *s* term. There is also a significant difference between 16:0 PC and 16:0–18:1 PC. This could be because 16:0 PC is in the gel phase at the temperature of analysis, whereas 16:0–18:1 PC is in the liquid crystalline phase. LSER data presented in Supplemental Figure 4 shows the solvation characteristics of 14:0 PC nanodiscs, for which the transition temperature is 24°C, at various temperatures. These analyses were conducted with 14:0 PC in the gel phase, liquid crystalline phase, and a mixture of the two phases because nanodiscs have a broad transition unlike liposomes[41]. As the nanodiscs transition from a liquid phase to a gel phase the only LSER parameter to change within standard error is the *s* term, which became more negative. These experiments suggest that the differences in the ability to interact with polar solutes observed between 16:0 PC and 16:0–18:1 PC can be attributed to the phase state of 16:0 PC which is considered to be a more ordered bilayer[42].

The *a* term for all of nanodiscs was positive implying that nanodiscs are more efficient hydrogen bond acceptors than the BGE. The structure of the polar head group must be considered to explain these results. Although the PC and SM head groups are polar, they each contain a quaternary ammonium with nonpolar methyl groups. As a result of these hydrophobic moieties, clathrate-like structures form wherein the polar water molecules form a lattice around the hydrophobic head groups[38,43,44]. This creates a hydration layer that can accept hydrogen bonds. In addition to this hydration layer the carbonyls on the phosphate and the ester groups are capable of accepting hydrogen bonds as well[35,36,38,45]. The *a* term for the nanodiscs composed of 16:0 PC was significantly more positive than all of the other nanodiscs with the exception of the nanodiscs composed of 14:0 PC. The *a* terms are not significantly different between 16:0 PC and 14:0 PC because they have the same head group chemistry and have saturated alkyl tails of a similar length. As can be seen in supplemental Figure 4, there is no difference between the *a* term of a lipid in the gel phase and a lipid in the liquid crystalline phase. The *a* terms for 14:1 PC and 16:0–18:1 PC are smaller than 16:0 PC. Fluorescence studies have shown that increased unsaturation in the alkyl tail region leads to weakened hydrogen bond interaction between the head groups[43], which may explain our observations. The 16:0 SM had significantly lower *a* term than 16:0 PC because of its ability to form intramolecular hydrogen bonds, reducing the ability of the carbonyls on the phosphate group to accept hydrogen bonds. The 0.8 14:0 PC 0.2 14:0 PS nanodisc has a significantly lower a term most likely due to the addition of 14:0 PS to the bilayer. Interestingly, there was a dramatic difference in the *a* term between the nanodisc that had a uniform 16:0 PC bilayer and the nanodisc of the mixed 0.75 16:0 PC and 0.25 14:0 PE. Phosphoethanolamine (PE) contains a primary ammonium instead of a quaternary ammonium. As a result of this change to the head group, PE lipids are capable of engaging in hydrogen bond donating with water and nonesterified oxygen on the phosphate group[38] and do not lead to formation of the clathrate structure. In addition to not forming a clathrate, PE head groups will break hydrogen bonds to undergo rotational motion[44]. These factors lead to a reduced ability to accept a hydrogen bond. The effects of changes in the *a* term on separation selectivity can be seen visually in the electropherogram in Figure 4.

Lastly the *b* term for all of the nanodiscs is negative because water in the BGE is a superior hydrogen bond donor. The only significant differences in the nanodisc LSER values were between 16:0–18:1 PC and 16:0 SM. The 16:0 SM *b* term was less negative than the 16:0–18:1 PC value and this is likely because of the structural differences between the head groups of the two lipids. At the interface between the hydrophobic and hydrophilic portion of the bilayer, 16:0 SM contains two moieties that are capable of donating a hydrogen bond[46], while the 16:0–18:1 PC contains only ester groups capable of accepting hydrogen bonds.

4. Conclusion

The properties of phospholipid and sphingomyelin nanodiscs were characterized using nanodisc EKC and LSER analysis. Increasing the Xiran 30010 to lipid ratio resulted in smaller, more cohesive nanodiscs with reduced retention of hydrogen bond donor solutes. Comparison of nanodiscs formed with two polymer belts, Xiran 30010 and Xiran 25010, determined either Xiran 30010 has greater affinity for hydrogen bond donating solutes or that Xiran 30010 produces structural changes in the bilayer that promote interaction with hydrogen bond donor molecules. LSER analysis showed that nanodisc EKC is sensitive to slight structural changes in lipid head group chemistry. Changes to in alkyl tail chemistry did not lead to significant changes in the bilayer-solute interactions because polar solutes rarely penetrate deep into the hydrophobic region. Comparison of LSER results for a nanodisc bilayer to published results for a lipid vesicle showed only minor differences that are likely due to differences in the lipid composition and bilayer curvature. Together, these results demonstrate that solute interactions with polymer-bound nanodiscs are primarily with, and representative of, interactions with the lipid bilayer. Nanodisc EKC has been shown as a reliable method for the measurement and characterization of bilayer-solute interactions.

Supplementary Material

Refer to Web version on PubMed Central for supplementary material.

Acknowledgments

The authors gratefully acknowledge financial support for this project from the Montana Research and Economic Development Initiative (grant number 51030-MUSRI2015-02) and NIH Award P20GM103546 to the Center for Biomolecular Structure and Dynamics at the University of Montana.

The authors gratefully acknowledge Stefan Scheidelaar and J. Antoinette Killian for the gift of the Xiran copolymers and useful discussions and advice on their use.

References

1. Terabe S, Otsuka K, Ichikawa K, Tsuchiya A, Ando T. Anal Chem. 1984; 56:111–113.
2. Terabe S, Otsuka K, Ando T. Anal Chem. 1985; 57(4):834–841.
3. Schnee VP, Palmer CP. Electrophoresis. 2008; 29(4):767–776. [PubMed: 18297644]
4. Rauk E, Kotzev A, Laschewsky A, Palmer CP. J Chromatogr A. 2006; 1106(1–2):29–35. [PubMed: 16443449]
5. Kopecká K, Tesašová E, Pirogov A, Gaš B. J Sep Sci. 2002; 25(15–17):1027–1034.
6. Klotz WL, Schure MR, Foley JP. J Chromatogr A. 2002; 962:207–219. [PubMed: 12198964]

7. Mohanty A, Dey J. J Chromatogr A. 2005; 1070(1–2):185–192. [PubMed: 15861803]
8. Poole SK, Patel S, Dehring K, Workman H, Dong J. J Chromatogr B Anal Technol Biomed Life Sci. 2003; 793(2):265–274.
9. Pomponio R, Gotti R, Luppi B, Cavrini V. Electrophoresis. 2003; 24(10):1658–1667. [PubMed: 12761797]
10. Ruokonen SK, Duša F, Lokajová J, Kilpeläinen I, King AWT, Wiedmer SK. J Chromatogr A. 2015; 1405:178–187. [PubMed: 26072299]
11. Wang Y, Sun J, Liu H, He Z. Electrophoresis. 2007; 28(14):2391–2395. [PubMed: 17578839]
12. Ruokonen SK, Duša F, Rantamäki AH, Robciuc A, Holma P, Holopainen JM, Abdel-Rehim M, Wiedmer SK. J Chromatogr A. 2017; 1479:194–203. [PubMed: 27955893]
13. Holland LA, Leigh AM. Electrophoresis. 2003; 24(17):2935–2939. [PubMed: 12973796]
14. Mills JO, Holland LA. Electrophoresis. 2004
15. Palmer CP, Keeffer A, Hilder EF, Haddad PR. Electrophoresis. 2011; 32(5):588–594. [PubMed: 21308694]
16. Hua X, Du Y, Chen J, Xu G, Yu T, Zhang Q. Electrophoresis. 2013; 34(13):1901–1907. [PubMed: 23592416]
17. McGettrick JR, Williamson NH, Sutton AT, Palmer CP. Electrophoresis. 2017; 38(5):730–737. [PubMed: 27869321]
18. Wiedmer SK, Holopainen JM, Mustakangas P, Kinnunen PKJ, Riekkola M. Electrophoresis. 2000; 21(15):3191–3198. [PubMed: 11001217]
19. Burns ST, Agbodjan AA, Khaledi MG. J Chromatogr A. 2002; 973(1–2):167–176. [PubMed: 12437175]
20. Wiedmer SK, Kulovesi P, Riekkola M. J Sep Sci. 2008; 31(14):2714–2721. [PubMed: 18693313]
21. Carrozzino JM, Khaledi MG. Pharm Res. 2004; 21(12):2327–2335. [PubMed: 15648265]
22. Penny WM, Steele HB, Ross JBA, Palmer CP. Electrophoresis. 2017; 38(5):738–746. [PubMed: 27859480]
23. Orwick MC, Judge PJ, Procek J, Lindholm L, Graziadei A, Engel A, Groebner G, Watts A. Angew Chemie - Int Ed. 2012; 51(19):4653–4657.
24. Knowles TJ, Finka R, Smith C, Lin YP, Dafforn T, Overduin M. J Am Chem Soc. 2009; 131(22): 7484–7485. [PubMed: 19449872]
25. Dörr JM, Koorengevel MC, Schäfer M, Prokofyev AV, Scheidelaar S, van der Cruijsen EAW, Dafforn TR, Baldus M, Killian JA. Proc Natl Acad Sci U S A. 2014; 111(52):18607–18612. [PubMed: 25512535]
26. Scheidelaar S, Koorengevel MC, Pardo JD, Meeldijk JD, Breukink E, Killian JA. Biophys J. 2015; 108(2):279–290. [PubMed: 25606677]
27. Dörr JM, Scheidelaar S, Koorengevel MC, Dominguez JJ, Schäfer M, van Walree CA, Killian JA. European Biophysics Journal. 2016:3–21. [PubMed: 26639665]
28. Pascoe RJ, Foley JP. Electrophoresis. 2003; 24(24):4227–4240. [PubMed: 14679570]
29. Swainsbury DJK, Scheidelaar S, Van Grondelle R, Killian JA, Jones MR. Angew Chemie - Int Ed. 2014; 53(44):11803–11807.
30. Bushey M, Jorgenson J. Anal Chem. 1989; 61:491–493.
31. Katz, E.Eksteen, R.Schoenmakers, P., Miller, N., editors. Handbook of HPLC. 1. M. Dekker; New York: 1998.
32. Hyslop JS, Hall LMG, Umansky AA, Palmer CP. Electrophoresis. 2014; 35(5):728–735. [PubMed: 24302072]
33. Hazel J. Prog Lipid Res. 1990; 29(3):167–227. [PubMed: 2131463]
34. Vitha M, Carr PW. J Chromatogr A. 2006; 1126(1–2):143–194. [PubMed: 16889784]
35. Lopez CF, Nielsen SO, Klein ML, Moore PB. J Phys Chem B. 2004; 108(21):6603–6610.
36. Tejwani RW, Davis ME, Anderson BD, Stouch TR. Mol Pharm. 2011; 8(6):2204–2215. [PubMed: 21988564]
37. Kim C, Baek S, Bin, Kim DH, Lim SC, Lee HJ, Lee HC. J Pept Sci. 2009; 15(5):353–358. [PubMed: 19189270]

38. Damodaran KV, Merz KM. Biophys J. 1994; 66(4):1076–1087. [PubMed: 8038380]
39. Marrink SJ, Berendsen HJC. J Phys Chem. 1996; 100(41):16729–16738.
40. Chiu SW, Vasudevan S, Jakobsson E, Mashl RJ, Scott HL. Biophys J. 2003; 85(6):3624–3635. [PubMed: 14645055]
41. Jamshad M, Grimard V, Idini I, Knowles TJ, Dowle MR, Schofield N, Sridhar P, Lin Y, Finka R, Wheatley M, Thomas ORT, Palmer RE, Overduin M, Govaerts C, Ruysschaert JM, Edler KJ, Dafforn TR. Nano Res. 2015; 8(3):774–789.
42. Essmann U, Perera L, Berkowitz ML. Langmuir. 1995; 11(24):4519–4531.
43. Slater SJ, Ho C, Taddeo FJ, Kelly MB, Stubbs CD. Biochemistry. 1993; 32(14):3714–3721. [PubMed: 8466911]
44. Damodaran KV, Merz KM. Langmuir. 1993; 9(5):1179–1183.
45. Norman KE, Nymeyer H. Biophys J. 2006; 91(6):2046–2054. [PubMed: 16815896]
46. Barenholz Y, Thompson TE. Biochim Biophys Acta - Biomembr. 1980; 604(2):129–158.

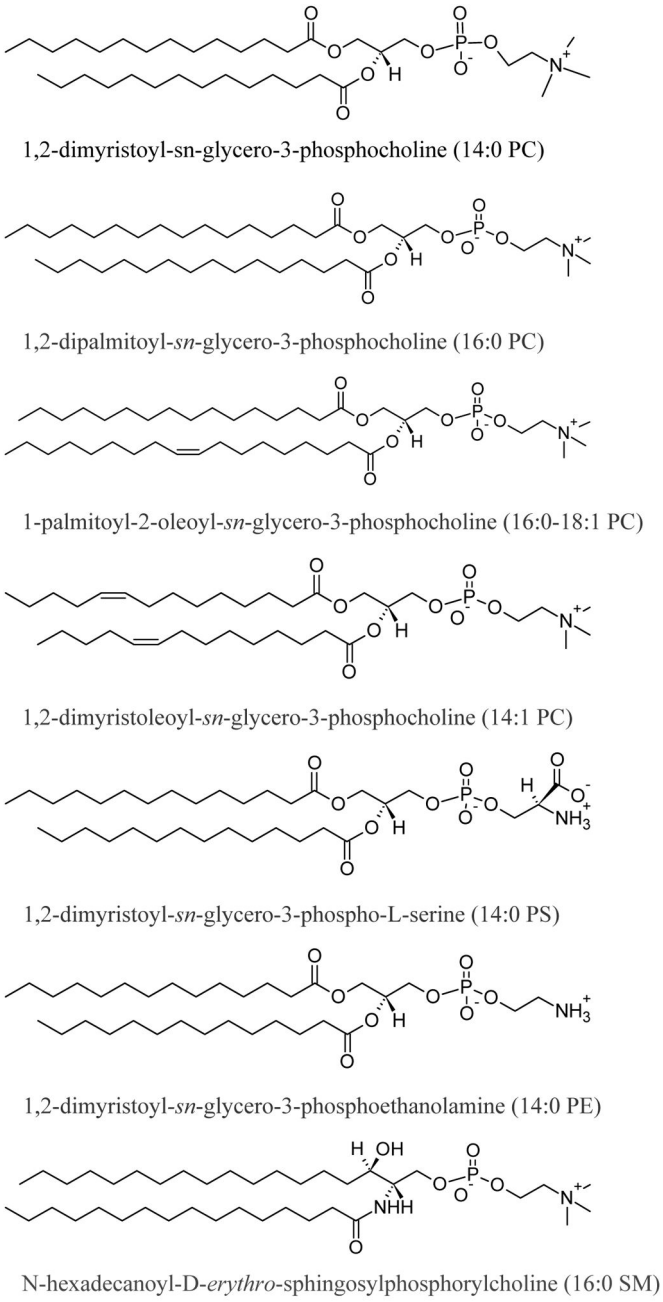

Figure 1.
Structures of lipids used

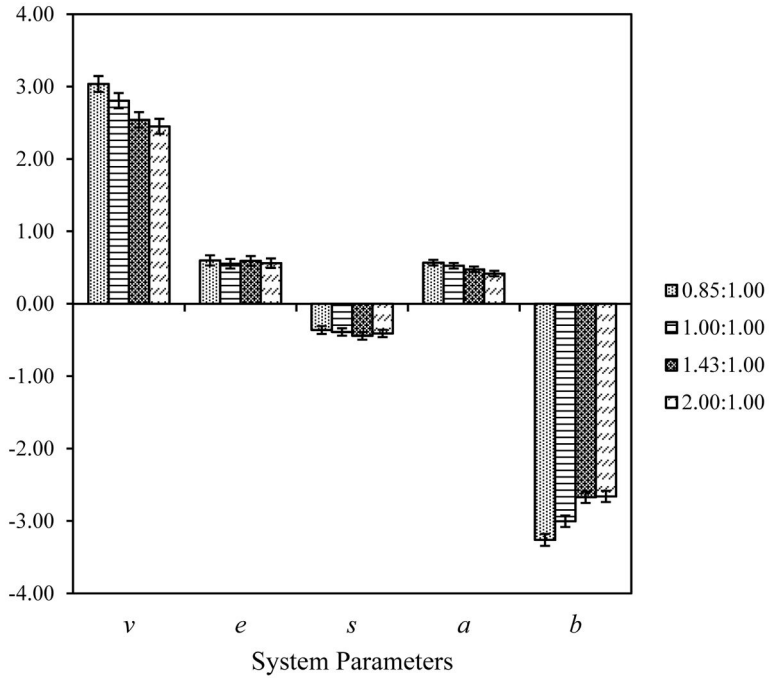

Figure 2.
Comparison of LSER parameters based on Xiran 30010 to 14:0 PC ratio

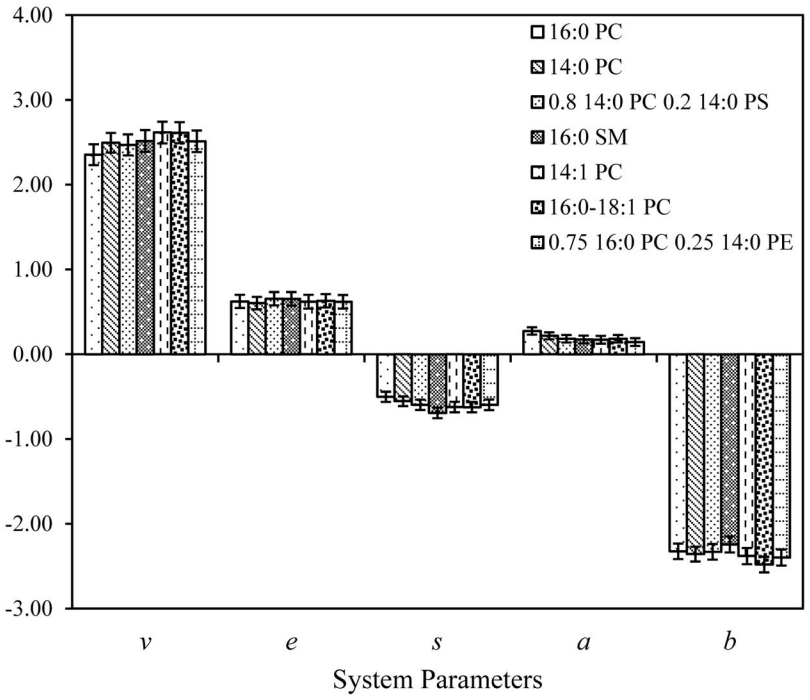

Figure 3.
Comparison of LSER results based on lipid composition

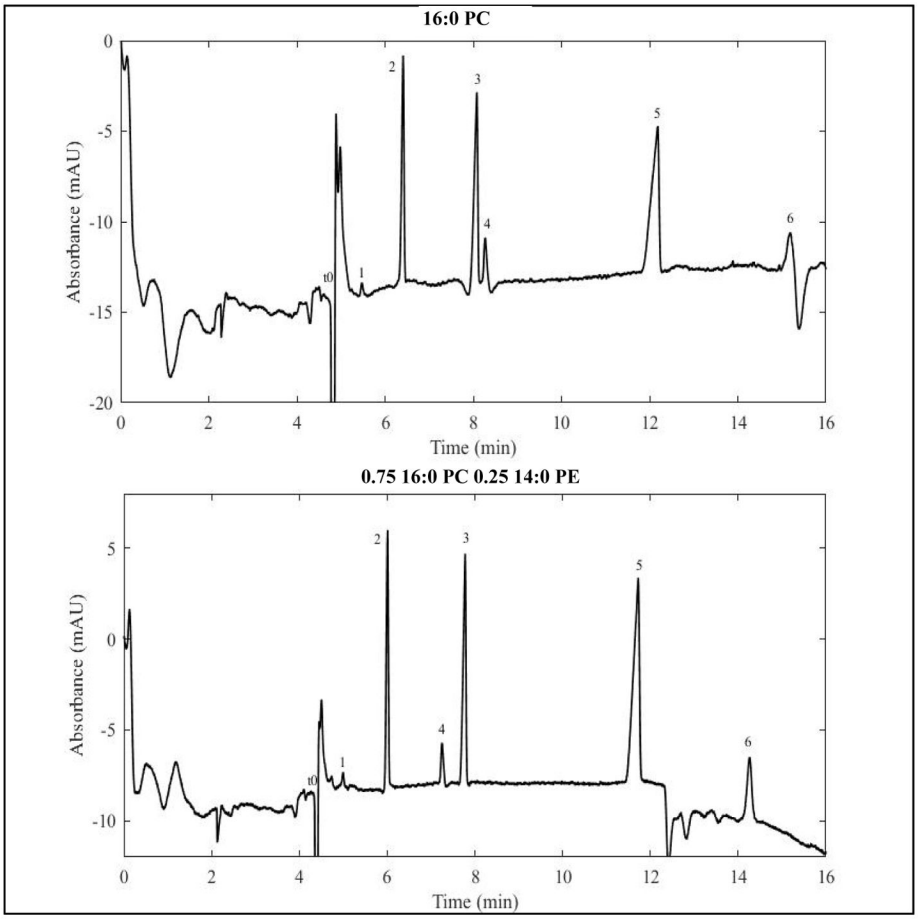

Figure 4.

Separation of six solutes: (1) Benzyl Alcohol, (2) Methyl Benzoate, (3) Ethyl Benzoate, (4) 4-Ethylphenol, (5) Propyl Benzoate, and (6) 4-Chlorotoluene. Separation parameters: 5 mM phospholipid nanodiscs with 2.50:1.00 (w:w) Xiran 25010 copolymer belt to lipid ratio, in a 25 mM phosphate pH 7.0. Capillary dimensions: 48.5 cm x 50μm I.D. with a 150μm extended cell pathlength. The injection was made with 35 mbar of pressure for 5 seconds. The operating voltage was 15 kV with detection at 245 nm. These separations averaged 169,000 theoretical plates

Table 1

Copolymer and lipid composition, experimental temperature, μ_{eo}, μ_{ep}, methylene selectivity, average theoretical plate count for the phenones used in the analysis, and the number of replicates of the experimental runs for lipid nanodiscs of systematically varied composition.

Copolymer	Copolymer: Lipid Ratio (w: w)	Nanodisc Lipid Composition	°C	μ_{eo} 10^4 (cm^2/V*s)	μ_{ep} 10^{-4} (cm^2/V*s)	α_{CH2}	N	n
30010	0.85:1.00	14:0 PC	25	4.46±0.15	−3.44±0.10	2.59±0.12	253,000±40,100	5
30010	1.00:1.00	14:0 PC	25	4.41±0.15	−3.49±0.03	2.56±0.04	259,000±26,600	6
30010	1.43:1.00	14:0 PC	25	4.05±0.25	−3.79±0.06	2.38±0.03	260,000±34,700	6
30010	2.00:1.00	14:0 PC	25	4.22±0.10	−3.76±0.01	2.33±0.01	298,000±34,500	4
25010	2.00:1.00	14:0 PC	24	4.36±0.06	−3.70±0.08	2.45±0.05	165,000±50,500	6
25010	2.50:1.00	14:0 PC	30	5.20±0.15	−4.12±0.03	2.37±0.03	256,000±39,300	6
25010	2.50:1.00	0.8 14:0 PC 0.2 14:0 PS	30	4.68±0.17	−4.10±0.05	2.39±0.06	201,300±34,200	6
25010	2.50:1.00	16:0 PC	30	4.53±0.08	−3.89±0.07	2.30±0.08	178,000±17,900	6
25010	2.50:1.00	0.75 16:0 PC 0.25 14:0 PE	30	5.00±0.06	−4.10±0.02	2.47±0.04	237,000±27,000	7
25010	2.50:1.00	16:0 SM	30	4.96±0.09	−4.09±0.03	2.37±0.03	232,000±24,300	7
25010	2.50:1.00	16:0–18:1 PC	30	4.89±0.09	−4.01±0.02	2.51±0.05	281,000±62,100	6
25010	2.50:1.00	14:1 PC	30	4.77±0.06	−4.02±0.04	2.44±0.03	222,000±9,600	5